Table 1 Mean C_T values and precision data of rtPCR and BD-Max assays

PCR target	Platform	Mean C_T at each dilution (CFU/mL)						Intra-assay		Inter-assay	
		10^8	10^6	10^3	10	0.1	0.01	SD	CV	SD	CV
B. pertussis IS481	rtPCR	12.97	22.62	25.53	33.69	34.51	35.28	1.38	5	3.74	5.04
	BD-Max	10.3	18.7	24.2	21.4	29.3	31	1.68	6.91	1.89	6.93
B. holmesii IS481	rtPCR	12.43	17.98	19.9	28.82	30.16	36.62	ND	ND	ND	ND
	BD-Max	16.4	29.4	24.9	29.35	36	33.4	ND	ND	ND	ND
B. holmesii hIS1001	rtPCR	11.54	17.66	23.76	36.84	37.87	37.03	0.02	0.1	0.02	0.09
	BD-Max	12.6	20.4	23.8	29.7	36.7	0	1.81	7.61	1.8	3.83
B. parapertussis pIS1001	rtPCR	33.23	36.5	37.84	38.29	40	0	1.19	3.07	1.09	2.81
	BD-Max	15.8	21.2	25.3	30.5	30.9	0	1.2	4.74	0.25	2.37
B. bronchiseptica IS481	rtPCR	12.07	18.75	22.6	26.92	28.05	35.46	ND	ND	ND	ND
	BD-Max	22.3	32.1	32.8	28.6	32.95	36.1	ND	ND	ND	ND

CFU, colony forming units; CV, co-efficient of variation (%); ND, not performed as these assays were not compared given low diagnostic value; SD, standard deviation.

This measure was higher than the intra- and inter-assay variability of the rtPCR.

Our findings demonstrated comparable performance of the rtPCR and BioGX BD-Max assays for the detection of *B. pertussis*, *B. holmesii* and *B. parapertussis*. Both assays were very sensitive in detecting *B. pertussis* and *B. holmesii.* The BioGX BD-Max assay was efficient and easy to use, however the rtPCR demonstrated higher specificity when detecting other *Bordetella* species. Further, the difference in cost per reportable analysis between the two assays was $21.30 for the BD-Max and $15.60 for the rtPCR which is an important consideration. These assays enable differentiation between relevant pathogenic species of *Bordetella* and improve the accuracy of public health notifications for pertussis.

Conflicts of interest and sources of funding: The authors state that there are no conflicts of interest to disclose.

Verlaine J. Timms[1,2], Winkie Fong[2], Neisha J. Jeoffreys[3], Vitali Sintchenko[1,2,3]

[1]Centre for Infectious Diseases and Microbiology — Public Health, Westmead Hospital, NSW, Australia; [2]Sydney Medical School, The University of Sydney, NSW, Australia; [3]Centre for Infectious Diseases and Microbiology Laboratory Services, NSW Health Pathology, Sydney, NSW, Australia

Contact Verlaine Timms, PhD.
E-mail: Verlaine.Timms@health.nsw.gov.au

1. Melvin JA, Scheller EV, Miller JF, *et al*. *Bordetella pertussis* pathogenesis: current and future challenges. *Nat Rev Microbiol* 2014; 12: 274–88.
2. Long SS, Lischner HW, Deforest A, *et al*. Serologic evidence of subclinical pertussis in immunized children. *Pediatr Infect Dis J* 1990; 9: 700–5.
3. Long SS, Welkon CJ, Clark JL. Widespread silent transmission of pertussis in families: antibody correlates of infection and symptomatology. *J Infect Dis* 1990; 161: 480–6.
4. Fong W, Timms V, Holmes N, *et al*. Detection and incidence of *Bordetella holmesii* in respiratory specimens from patients with pertussis-like symptoms in New South Wales, Australia. *Pathology* 2018; 50: 322–6.
5. Mattoo S, Cherry JD. Molecular pathogenesis, epidemiology, and clinical manifestations of respiratory infections due to *Bordetella pertussis* and other Bordetella subspecies. *Clin Microbiol Rev* 2005; 18: 326–82.
6. Glare EM, Paton JC, Premier RR, *et al*. Analysis of a repetitive DNA sequence from *Bordetella pertussis* and its application to the diagnosis of pertussis using the polymerase chain reaction. *J Clin Microbiol* 1990; 28: 1982–7.
7. Loeffelholz MJ, Thompson CJ, Long KS, *et al*. Detection of *Bordetella holmesii* using *Bordetella pertussis IS481* PCR assay. *J Clin Microbiol* 2000; 38: 467.
8. Tatti KM, Sparks KN, Boney KO, *et al*. Novel multitarget real-time PCR assay for rapid detection of Bordetella species in clinical specimens. *J Clin Microbiol* 2011; 49: 4059–66.
9. Cloud JL, Hymas WC, Turlak A, *et al*. Description of a multiplex *Bordetella pertussis* and *Bordetella parapertussis* LightCycler PCR assay with inhibition control. *Diagn Microbiol Infect Dis* 2003; 46: 189–95.
10. Kenicer J, Hardie A, Hamilton F, *et al*. Comparative evaluation of the Diagenode multiplex PCR assay on the BD max system versus a routine in-house assay for detection of *Bordetella pertussis*. *J Clin Microbiol* 2014; 52: 2668–70.
11. Octavia S, Sintchenko V, Gilbert GL, *et al*. Newly emerging clones of Bordetella pertussis carrying prn2 and ptxP3 alleles implicated in Australian pertussis epidemic in 2008-2010. *J Infect Dis* 2012; 205: 1220–4.
12. Poddar SK. Detection and discrimination of *B pertussis* and *B holmesii* by real-time PCR targeting *IS481* using a beacon probe and probe-target melting analysis. *Mol Cell Probes* 2003; 17: 91–8.
13. Rodgers L, Martin SW, Cohn A, *et al*. Epidemiologic and laboratory features of a large outbreak of pertussis-like illnesses associated with cocirculating *Bordetella holmesii* and *Bordetella pertussis*–Ohio, 2010-2011. *Clin Infect Dis* 2013; 56: 322–31.

DOI: https://doi.org/10.1016/j.pathol.2018.10.018

Malignant gastrointestinal neuroectodermal tumour (GNET): neural mesenchymal tumours of the gastrointestinal tract with striking histology and *EWSR1* gene rearrangement

Sir,

Malignant gastrointestinal neuroectodermal tumours (GNET) are rare primitive mesenchymal neoplasms of the tubular gut previously considered to be gastrointestinal manifestations of soft tissue clear cell sarcomas (CCS). While both entities share a recurrent balanced translocation profile involving the

Ewing sarcoma breakpoint region 1 (*EWSR1*) gene on chromosome 22 and the presence of a clear cell component on histology, there are distinctive morphological and immunophenotypic features which distinguish the two. In this report, we present a small bowel GNET case and review the literature regarding these unusual mesenchymal neoplasms.

A 53-year-old male presented with sudden onset acute abdominal pain. His background was unremarkable apart from epilepsy which was well controlled on medication and mild intermittent periumbilical discomfort of one year duration, for which he underwent endoscopic evaluation which detected no abnormality. Imaging by computed tomography revealed a small bowel mass with significant extramural heterogeneous inflammation suspicious for abscess formation, and mild proximal bowel dilatation suggestive of partial obstruction. His blood and clinical biochemistry results were within normal limits (including serum tumour markers CA125, CA19.9 and CEA). He was hospitalised for a short course of intravenous antibiotics with symptomatic improvement. The patient was discharged and underwent an elective laparoscopic exploration with segmental small bowel resection two months later.

The surgical specimen comprised a segment of small bowel with a 30 mm partly stenotic annular tumour involving much of the bowel wall (see Fig. 1). No significant lymphadenopathy was noted macroscopically. Haematoxylin and eosin (H&E) sections revealed a tumour composed of ovoid/epithelioid and spindled cells arranged in geographic sheets with part pushing and part infiltrating borders. There was transmural involvement including the mucosa, submucosa, muscularis propria and subserosa. There was patchy intratumoural necrosis with mitotic activity numbering up to 10/10HPF.

The spindle cells were predominantly arranged in sweeping and variably intersecting fascicles, however a range of architectural patterns were observed in the ovoid/epithelioid cell areas, including pseudopapillary, pseudoalveolar and microcystic change. Focal clear cell change (mainly in areas with microcystic change) and abortive rosette formations were noted. Intra-tumoural multinucleate giant cells were not identified. A mesenteric lymph node showed a subcapsular metastatic deposit with identical histomorphology to the main tumour. The histological features are presented in Fig. 2.

On immunohistochemistry, the tumour cells showed strong diffuse expression of S100 (cytoplasmic only), SOX10 and CD56. Synaptophysin was patchy and of weak to moderate intensity, while chromograninA was negative. HMB45, melanA, CD34, DOG1, SMA, desmin, CD31 and cytokeratins AE1/AE3 and CK8/18 (CAM5.2) were negative.

In view of the striking histology, neural immunophenotype and absence of melanocytic differentiation, a provisional diagnosis of GNET was rendered. Our list of diagnostic differentials included an unusual gastrointestinal stromal tumour (excluded by the lack of CD117 and DOG1 expression), metastatic melanoma or soft tissue clear cell sarcoma (excluded by absence of melanocytic differentiation on immunohistochemistry), and malignant peripheral nerve sheath tumour (unlikely given the overall strong diffuse expression of neural markers and distinctive histology). A representative tumour block was submitted for interphase fluorescent *in situ* hybridisation, where *EWSR1* gene rearrangement was confirmed in a significant number of tumour cells (>50%) using the Vysis *EWSR1* break-apart probe.

GNETs were previously known as clear cell sarcoma-like tumour (with osteoclast-like giant cells[1]) of the gastrointestinal tract given their overlapping histological, immunophenotypical and molecular features with soft tissue clear cell sarcomas. Unlike the soft tissue sarcomas, however, melanocytic differentiation is consistently absent. In their seminal case series, Stockman and colleagues demonstrated the presence of dense secretory core granules by electron microscoscopy, a characteristic neural/neurosecretory phenotype.[2] Melanosome bodies were not identified. The authors postulated that GNETs arise from neural crest progenitor cells of the gastrointestinal tract autonomic system. This primitive lineage may explain in large part the spectrum of histology seen in these tumours, including neural rosette-like structures.

Rarely, GNET may show patchy oncocytic change, a potential diagnostic pitfall. Boland *et al.* recently described a GNET in the stomach of a 49-year-old woman which was initially misdiagnosed as malignant granular cell tumour on biopsy due to striking oncocytosis of the neoplastic cells.[3] The subsequent resection specimen revealed more conventional GNET areas.

GNETs and CCS share a recurrent balanced translocation involving *EWSR1* on chromosome 22 and one of either partners: *cAMP dependent activating transcription factor 1* (*ATF1*) on chromosome 12 or less commonly, *cAMP responsive element binding protein 1* (*CREB1*) located on chromosome 2.[4,5] The resulting chimaeric fusion proteins are postulated to activate downstream genes such as

Fig. 1 Segmental small bowel resection specimen post formalin fixation. The annular tumour displayed firm tan cut surfaces and showed transmural involvement with extension into mesenteric adipose tissue.

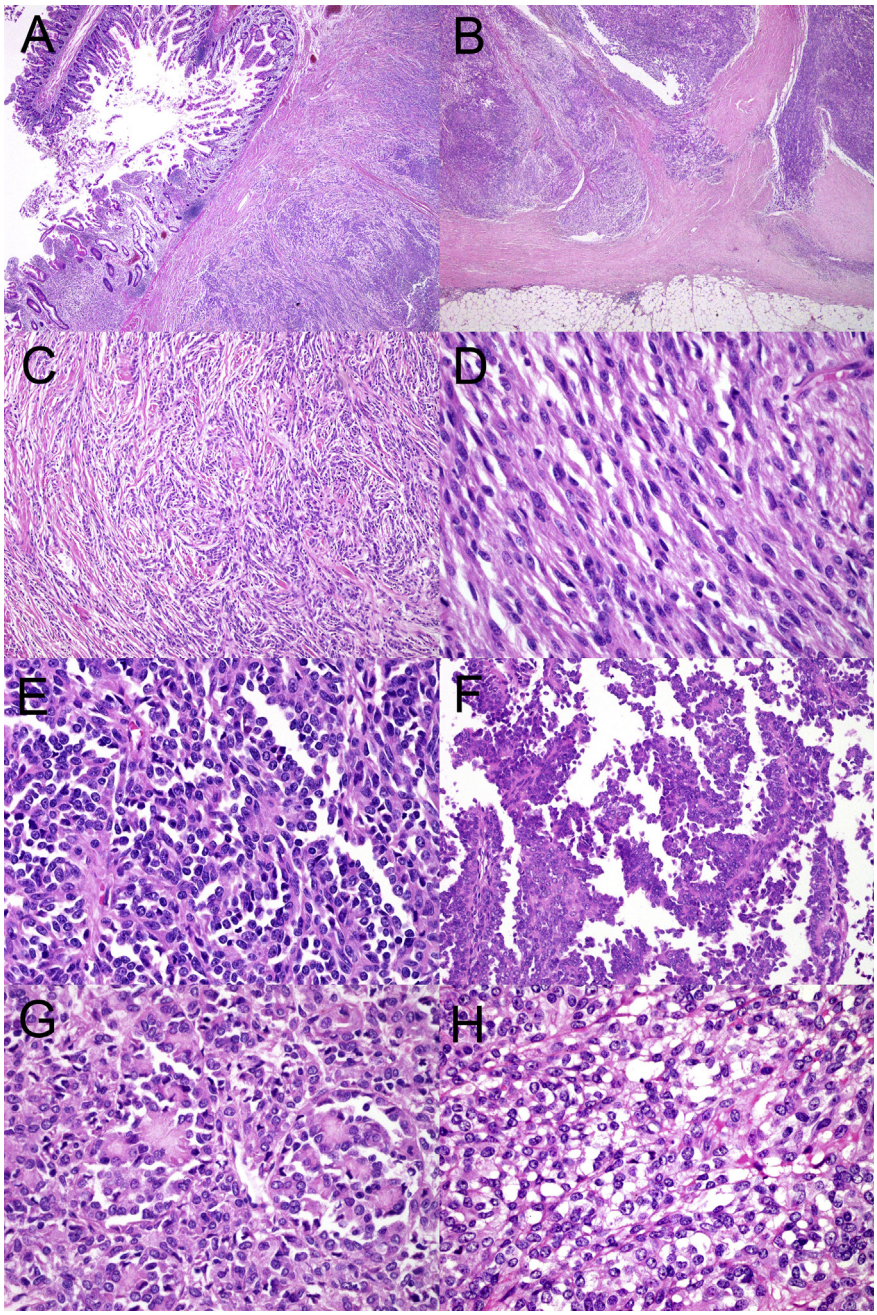

Fig. 2 Tumour cells involved the mucosa, submucosa and small bowel wall with part pushing and infiltrating borders (A,B). The component cells were spindled (C,D) and ovoid/epithelioid where a spectrum of growth patterns including pseudoalveolar (E), pseudopapillary (F) features were seen. Abortive rosette-like structures were noted (G), and focal clear cell change was present (H).

Microopthalmia transcription factor 1 (*MiTF1*) which drive melanocytic phenotypic differentiation and survival. The absence of a melanocytic immunophenotype in GNETs (despite sharing these molecular translocations) suggests additional molecular alterations which may be unique to, and further define, GNETs. As the *EWSR1-ATF1* gene fusion can also be found in a variety of unrelated soft tissue tumours, such as hyalinising clear cell sarcoma of the salivary gland[6] and angiomatoid fibrous histiocytoma[7] (where *EWSR1-CREB1* gene fusion is also detected), molecular testing should always be performed in the context of anatomical pathology considerations.

The published literature on GNET remains sparse. In the case series by Stockman *et al.*, six of twelve patients were dead with disease two-and-a-half years after initial diagnosis, with the remainder alive with metastatic disease. A recent description of a clinically indolent rectal GNET (after 10 years of follow-up post-curative resection) exists, although the authors note that only ~2% of neoplastic cells showed *EWSR1* gene rearrangement.[8] Our patient is being managed expectantly and remains alive without radiological evidence of disease recurrence at the time of writing six months after surgery.

In summary, we describe a rare case of GNET of the small bowel in an adult male presenting with an acute abdomen due

to tumoural obstructive symptoms. His clinical history was unremarkable for malignancy. GNETs occur in young to middle aged adults without a gender predilection. They are composed of varying proportions of spindled and ovoid/epithelioid cells which can show a spectrum of histological architectural features in the epithelioid component. Multinucleate giant cells are variably present, clear cell change may be focal, and oncocytosis may rarely be seen. The immunophenotype is neural, melanocytic differentiation is absent, and there is consistent detection of *EWSR1* gene rearrangement with fusion partners *ATF1* or *CREB1* by *in situ* hybridisation. GNETs are postulated to arise from primitive neural crest progenitor cells of the gastrointestinal tract autonomic nervous system. The prognosis appears poor, although published data with follow-up information is scant, given the rarity of this disease.

Conflicts of interest and sources of funding: The authors state that there are no conflicts of interest to disclose.

Christopher W. Toon[1,2,3], Wendy Cooper[2,4,5], Christina Selinger[4], Christophe R. Berney[6], Jeanne Tomlinson[7]

[1]Histopath Diagnostic Specialists, Macquarie Park, NSW, Australia; [2]Sydney Medical School, University of Sydney, Sydney, NSW, Australia; [3]Cancer Diagnosis and Pathology Group, Kolling Institute of Medical Research, St Leonards, NSW, Australia; [4]Department of Tissue Pathology and Diagnostic Oncology, Royal Prince Alfred Hospital, Camperdown, NSW, Australia; [5]School of Medicine, Western Sydney University, Sydney, NSW, Australia; [6]University of NSW, Department of Surgery, Bankstown-Lidcombe Hospital, Bankstown, NSW, Australia; [7]Laverty Pathology, North Ryde, NSW, Australia

Contact Dr Christopher W. Toon.
E-mail: ctoon@med.usyd.edu.au

1. Friedrichs N, Testi MA, Moiraghi L, *et al*. Clear cell sarcoma-like tumor with osteoclast-like giant cells in the small bowel: further evidence for a new tumor entity. *Int J Surg Pathol* 2005; 13: 313–8.
2. Stockman DL, Miettinen M, Suster S, *et al*. Malignant gastrointestinal neuroectodermal tumor: clinicopathologic, immunohistochemical, ultrastructural, and molecular analysis of 16 cases with a reappraisal of clear cell sarcoma-like tumors of the gastrointestinal tract. *Am J Surg Pathol* 2012; 36: 857–68.
3. Boland JM, Folpe AL. Oncocytic variant of malignant gastrointestinal neuroectodermal tumor: a potential diagnostic pitfall. *Hum Pathol* 2016; 57: 13–6.
4. Kosemehmetoglu K, Folpe AL. Clear cell sarcoma of tendons and aponeuroses, and osteoclast-rich tumour of the gastrointestinal tract with features resembling clear cell sarcoma of soft parts: a review and update. *J Clin Pathol* 2010; 63: 416–23.
5. Antonescu CR, Nafa K, Segal NH, *et al*. EWS-CREB1: a recurrent variant fusion in clear cell sarcoma—association with gastrointestinal location and absence of melanocytic differentiation. *Clin Cancer Res* 2006; 12: 5356–62.
6. Antonescu CR, Katabi N, Zhang L, *et al*. EWSR1-ATF1 fusion is a novel and consistent finding in hyalinizing clear-cell carcinoma of salivary gland. *Genes Chromosomes Cancer* 2011; 50: 559–70.
7. Rossi S, Szuhai K, Ijszenga M, *et al*. EWSR1-CREB1 and EWSR1-ATF1 fusion genes in angiomatoid fibrous histiocytoma. *Clin Cancer Res* 2007; 13: 7322–8.
8. Prado G, Gorcey SA, Szallasi A, *et al*. Indolent gastrointestinal neuroectodermal tumor (GNET) of the colon: a new entity. *J Gastrointest Cancer Stromal Tumor* 2017; 2: 2.

DOI: https://doi.org/10.1016/j.pathol.2018.09.066

Androgen receptor immunoexpression in triple-negative breast cancers: is it a prognostic factor?

Sir,

Breast cancer is a heterogenous group of carcinomas with distinct clinical outcomes and therapeutic paradigms depending on their specific molecular profiles. Triple negative breast cancers (TNBCs) exhibit aggressive behaviour and are defined by the absence of oestrogen receptor, progesterone receptor and human epidermal growth factor 2 (HER2) overexpression. TNBCs display diverse molecular phenotypes with differing clinical characteristics and have recently been refined into four molecular subtypes: basal-like 1, basal-like 2, mesenchymal, and luminal androgen receptor-like (LAR).[1] Because TNBCs have less favourable outcomes and lack specific targeted therapy, there have been increasing efforts to identify potential prognostic and predictive markers in TNBCs.

Many breast cancers express androgen receptor (AR) and there has been recent interest in the role of AR as a potential biomarker in TNBCs. Approximately 10–35% of TNBCs express AR[2,3] when using a threshold of 10% nuclear staining by immunohistochemistry (IHC). AR expression has been demonstrated to confer an improved outcome in ER positive breast cancers and has been shown to be associated with smaller tumour size, lower clinical stage and lower mitotic score.[2,4–6] However, the role of AR in TNBCs is less clear. Some studies have suggested AR expression is associated with a favourable outcome in TNBCs[3,5,6] including response to anti-androgen therapy such as enzalutamide.[7] However, other studies have found no difference[8] or even a negative prognostic impact of AR expression, with increased mortality and poorer outcomes in ER negative breast cancers.[9] Therefore, we sought to investigate the clinical and pathological associations of AR expression in a large unselected cohort of Australian patients with TNBC.

A tissue microarray (TMA) of consecutive primary triple negative breast carcinoma cases reported at Department of Anatomical Pathology, Royal North Shore Hospital, Sydney, was used. These cases had undergone resection between 2005 and 2015. Metastases, core biopsy specimens and cases occurring in males were excluded. The TMA contained two 1 mm cores from each tumour. Androgen receptor immunohistochemistry was performed using a commercially available rabbit polyclonal antibody (clone SP107; dilution 1/50, after heat induced antigen retrieval in an alkaline retrieval solution; Cell Marque, USA).

Greater than or equal to 10% nuclear staining was classified as positive (Fig. 1). The TMAs were scored by two independent observers and AR IHC was repeated on whole tissue sections in cases which demonstrated equivocal staining or when there was discordance between the two observers. Statistical analysis was performed using SPSS version 24.0 (Statistical Package for Social Sciences, USA). AR expression was correlated with other prognostic factors, using paired t-test and Pearson's Chi-square test.

AR expression was also correlated with disease free survival (DFS) and overall survival (OS). OS was measured from the date of surgery to the date of death or last available